Mice lacking tartrate-resistant acid phosphatase (Acp 5) have disrupted endochondral ossification and mild osteopetrosis

Alison R. Hayman[1], Sheila J. Jones[2], Alan Boyde[2], Diane Foster[3], William H. Colledge[3], Mark B. Carlton[3], Martin J. Evans[3] and Timothy M. Cox[1],*

[1]Department of Medicine, University of Cambridge, Level 5, Addenbrooke's Hospital, Cambridge CB2 2QQ, UK
[2]Department of Anatomy and Developmental Biology, University College, London, Gower Street, London WC1E 6BT, UK
[3]Wellcome Trust/Cancer Research Campaign Institute of Cancer and Developmental Biology and Department of Genetics, University of Cambridge, Cambridge CB2 1QR, UK

*Author for correspondence

SUMMARY

Mature osteoclasts specifically express the purple, band 5 isozyme (Acp 5) of tartrate-resistant acid phosphatase, a binuclear metalloenzyme that can generate reactive oxygen species. The function of Acp 5 was investigated by targeted disruption of the gene in mice. Animals homozygous for the null *Acp 5* allele had progressive foreshortening and deformity of the long bones and axial skeleton but apparently normal tooth eruption and skull plate development, indicating a rôle for Acp 5 in endochondral ossification. Histomorphometry and mineralization density analysis of backscattered electron imaging revealed widened and disorganized epiphyseal growth plates with delayed mineralization of cartilage in 6- to 8-week-old mutant mice. The membrane bones of the skull showed increased density at all ages examined, indicating defective osteoclastic bone turnover. Increased mineralization density was observed in the long bones of older animals which showed modelling deformities at their extremities: heterozygotes and homozygous *Acp 5* mutant mice had tissue that was more mineralized and occupied a greater proportion of the bone in all regions. Thus the findings reflect a mild osteopetrosis due to an intrinsic defect of osteoclastic modelling activity that was confirmed in the resorption pit assay in vitro. We conclude that this bifunctional metalloprotein of the osteoclast is required for normal mineralization of cartilage in developing bones; it also maintains integrity and turnover of the adult skeleton by a critical contribution to bone matrix resorption.

Key words: mouse, tartrate, acid phosphatase, ossification, osteopetrosis, Acp 5

INTRODUCTION

Osteoclasts originate from myeloid progenitor cells (Joterau and Le Douarin, 1978; Roodman et al., 1985) and migrate to the skeleton where they participate in bone development and remodelling throughout life (Erlebacher et al., 1995). Long bones form within mesenchymal cartilage which is mineralized before it is resorbed by osteoclasts and replaced by bone matrix. In adult bones, osteoclasts participate in the remodelling cycle which is initiated by resorption of discrete areas of mineralized bone matrix. These are reinstated functionally, but not necessarily positionally, by compensatory formation of new bone that originates from mesenchymally derived osteoblasts and osteocytes. An imbalance between the rate of resorption of bone by osteoclasts and the co-ordinated renewal of bone by osteoblasts causes either osteopetrosis (excessive mineralization and consolidation) or osteoporosis (with trabecular loss) (Marks and Walker, 1976; Parfitt, 1994). The nature of the stimuli that activate osteoclasts and the means by which they degrade mineralized cartilage and bone matrix are unknown. Nonetheless, a better understanding of the processes that regulate bone metabolism and osteoclast function should shed light on pathological disorders, such as osteoporosis – a common affliction of the human skeleton (Manolagas and Jilka, 1995).

Osteoclasts specifically express the band 5 isozyme of tartrate-resistant acid phosphatase, Acp 5 (EC 3.1.3.2) (Minkin, 1982). This is a binuclear iron protein of unknown function that is secreted into the resorptive vacuole underlying the activated osteoclast (Reinholt et al., 1990) and is increased in the plasma when bone remodelling is active (Lau et al., 1987; Chamberlain et al., 1995). The Acp 5 isozyme promotes the hydrolysis of nucleotides, arylphosphates and phosphoproteins (Hayman et al., 1989; Nash et al., 1993) and is defined by its unique cathodal mobility at pH4 and resistance to inhibition by L(+) tartrate (Li et al., 1970). Recent studies have shown that tartrate-resistant acid phosphatase from rat osteoclasts partially dephosphorylates the bone matrix phosphoproteins, osteopontin and bone sialoprotein; after modification, these proteins are no longer permissive for osteoclast attachment (Ek-Rylander et al., 1994). It is thus plausible that Acp 5 influences the phosphorylation status of critical proteins of the bone matrix that bind hydroxyapatite and are associated with regions of bone formation.

Lately, superoxide and other reactive oxygen species have been implicated in bone resorption: not only do these radicals enhance recruitment of osteoclasts but reactive oxygen species are released at the ruffled membrane interface with bone (Garrett et al., 1990; Key et al., 1994). Osteoclasts, like other cells derived from granulocyte-monocyte progenitors in the bone marrow, possess NADPH oxidase which catalyses super-oxide production in situ during active bone resorption (Steinbeck et al., 1994) and free radical generation has been shown to reflect hormone- and cytokine-induced stimulation of matrix degradation by cultured osteoclasts (Garrett et al., 1990). Acp 5, the tartrate-resistant acid phosphatase of osteo-clasts, is a member of a widely distributed class of purple proteins that contain a unique Fe^{2+}/Fe^{3+} metal centre (Que and Scarrow, 1988), which is able to catalyse hydroxyl radical formation (Sibille et al., 1987). Since this metalloprotein is co-secreted with superoxide into the resorptive vacuole of the activated osteoclast, and catalyses peroxidation reactions, Hayman and Cox proposed that it also participates in special-ized electrochemical reactions associated with resorption of bone matrix by the osteoclast (Hayman and Cox, 1994).

To explore the physiological action and developmental rôle of bifunctional tartrate-resistant acid phosphatase in the osteo-clast, we have generated mice that harbour a non-functional allele of *Acp 5* using targeted homologous recombination in murine embryonic stem cells. These mice mature normally but exhibit developmental and modelling deformities of the limb bones and axial skeleton. Histomorphometric and backscat-tered electron image analysis revealed disturbances in the cal-cification of the cartilaginous matrix and increased mineralized tissue density in membrane bones and all regions of the long bones. Acp 5 thus participates in the early stages of endo-chondral ossification and also plays a crucial part in osteo-clastic resorption of bone matrix: these distinct physiological rôles may reflect the bifunctional chemical properties of the purple acid phosphatases.

MATERIALS AND METHODS

Generation of mice with targeted disruption of *Acp 5*

To generate the targeting plasmid, a 4350 bp *Mun*I-*Sst*I *Acp 5* fragment isolated from a 129 mouse genomic library in λEMBL 3, was ligated into the corresponding sites of the pBluescript SK vector. Selection of embryonic stem cells that had undergone homologous recombination was facilitated by insertion of a *Pgk neo* cassette (Mansour et al., 1988) that was released by *Hin*dIII-*Eco*RI digestion from pKJ1 and blunt-ligated into the unique *Bgl*II site in exon 2 of the *Acp 5* coding region (Cassady et al., 1993) within the conserved putative iron-binding domain (Lord et al., 1990) to generate *Acp 5* (neo). A 2030 bp *Bam*HI-*Hin*dIII *tk* fragment from pSP64, driven by a modified HSV promoter (Pevny et al., 1991), was subcloned into the *Sac*I site of *Acp 5* (neo) to generate the 11183 bp targeting vector, Acp 5(neo)tk, which was linearized by digestion with *Hin*dIII.

5 μg of linearized Acp 5(neo)tk construct DNA was electroporated into CCB embryonic stem (ES) cells and clones resistant to both G418 (250 μg/ml) and gancyclovir (2 μM) were expanded and screened for targeted gene disruption (Evans, 1994). The predicted genomic structure of the disrupted allele was indicated by Southern blot analysis using an upstream 1.08 hybridization probe obtained as a *Bgl*I-*Nsi*I genomic fragment whose sequence is not present in the targeting vector. Digestion with *Bgl*I generated a 5.5 kb hybridizing genomic fragment, resulting from the targeting event and due to the

presence of a *Bgl*I site in the *Pgk neo* sequence (Fig. 1A). Hybridiz-ation with a full-length *Acp 5* cDNA probe, using restriction digests with *Stu*I, similarly confirmed the predicted locus (Cassady et al., 1993), not shown.

Cells from two of the four independently targeted ES cell clones (Fig. 1B) were injected into 3.5 day post-coitus C57BL/6 host blas-tocysts that were then implanted into pseudopregnant foster female mice (Evans, 1994). Germ-line transmission of the ES cell genome was monitored by inspection for agouti coat colour and by Southern blot hybridization analysis using genomic DNA obtained by tail biopsy to detect transmission of the disrupted *Acp 5* locus (Fig. 1C). Mice heterozygous for the disrupted *Acp 5* allele (*Acp 5* +/−) were
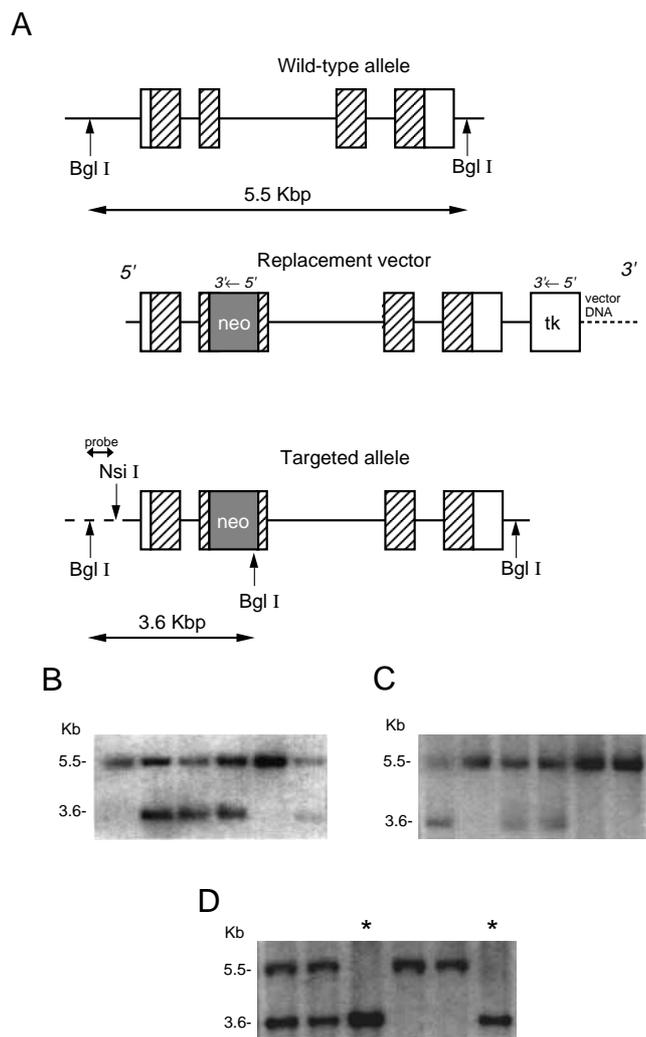
Fig. 1. Targeted disruption of the murine *Acp 5* gene. (A) Structure of the *Acp 5* gene, the replacement vector, Acp 5 (neo)tk and the predicted structure of the targeted *Acp 5* locus following homologous recombination. (B) Detection of *Acp 5* targeted ES clones. DNA from ES samples was digested with *Bgl*I, separated in agarose and transferred to Hybond N+ membranes for hybridization with the designated flanking probe. Wild-type alleles are represented by 5.5 kb and mutant alleles by 3.6 kb *Bgl*I restriction fragments. (C) Germ-line transmission of *Acp 5* mutant alleles confirmed by Southern blot hybridization analysis of DNA obtained from tail biopsies. (D) Genotyping of members of a litter obtained from an intercross between *Acp 5* +/− heterozygotes. Mouse tail DNA was digested with *Bgl*I and analysed by Southern blot hybridization with the probe as shown in A. Homozygous *Acp 5* mutants are indicated by asterisk.

crossed to obtain animals homozygous for the mutation (*Acp 5 –/–*), Fig. 1D.

Assay of type 5 acid phosphatase activity

Femurs were removed immediately after death and dissected free of muscle. The individual bones were minced and homogenized in 0.4 M sodium acetate, pH 5.6 containing 2% ^{w}/v Triton X-100. To assay specifically for band 5 acid phosphatase in osteoclasts, immunoabsorption with immobilized rabbit antibodies to porcine uteroferrin was carried out (Echetebu et al., 1987) after neutralizing 13,000 **g** supernatant bone extracts to pH 7.5 with Tris base. Tartrate-resistant acid phosphatase activity was finally determined spectrophotometrically before and after immunoabsorption in the presence of 0.1 M L(+) sodium tartrate at pH 5.6 using 10 mM 4-nitrophenyl phosphate as substrate (Hayman et al., 1989).

Radiographs and histology

Mice were briefly narcotised to facilitate radiography. For comparative purposes, high-resolution Kodak mammography X-ray film was employed and identical radiation energy (45 kV) and photographic exposures were used to prepare radiographs on separate portions of the same film. After killing, bones were fixed in 10% buffered formol saline and decalcified in dilute citric acid for 5 days, dehydrated and embedded in paraffin wax. Sections (4 μm) were cut and stained with alcian blue and picrofuchsin.

Morphological study using scanning electron microscopy

The histology of the tissues was also examined using embedded, micromilled specimens and backscattered electron imaging as described below.

Longitudinally sectioned tail vertebrae and long bones and entire mandibles were prepared for conventional 3D morphological imaging in scanning electron microscopy, using secondary electron and backscattered electron modes. The bones were cleaned and rendered superficially "anorganic" (i.e. unmineralized tissue was removed selectively) using solutions of sodium hypochlorite. These samples were washed, dehydrated with ethanol, air-dried and coated with carbon.

Quantification of bone mineral density

The distribution of mineralization densities within the calcified tissues was examined by backscattered electron microscopy (BSE-SEM) quantified by digital image analysis (Boyde et al., 1995a,b).

Freshly dissected bones obtained from age- and sex-matched 129 strain mice of defined *Acp 5* genotype were fixed in 70% ^{w}/v ethanol, dissected free of bulk soft tissue, dehydrated in ethanol and embedded in poly-methyl-methacrylate (PMMA). Block faces were cut through the specimens, diamond micromilled, coated with carbon and analysed using backscattered electrons (BSE) in a digital scanning electron microscope (SEM; Zeiss DSM962, equipped with an annular solid state BSE detector, KE Electronics, Toft, Cambs, UK: Boyde et al., 1995a), operated at 20 kV and 0.5 nA. The mineralization density of the calcified tissues was determined by comparison with halogenated dimethacrylate standards (Boyde et al., 1995b). The proportion of bone or calcified cartilage falling into each of 8 equal intervals from $C_{22}H_{25}0_{10}Br$ (mean BSE coefficient calculated by the procedure given by Lloyd (1987) = 0.1159) to $C_{22}H_{25}0_{10}I$ (mean BSE coeff. 0.1519) was calculated. For presentation of the digital images, the same eight intervals were represented by a pseudocolour scheme.

Mandibles from 12-week-old +/+, +/– and –/– mice were embedded in PMMA, and the blocks trimmed and micromilled to provide nearly midline longitudinal sections of the incisors and molars. Calvaria were obtained from 7-day-old; and 3-, 6-, 7- and 13-month-old Acp 5 –/– mice that were age- and sex-matched to congenic control Acp 5 +/+ animals and embedded for mid-parietal coronal or anteroposterior sectioning. For the BSE analysis, the mineralization densities of dentine and enamel were related to the range
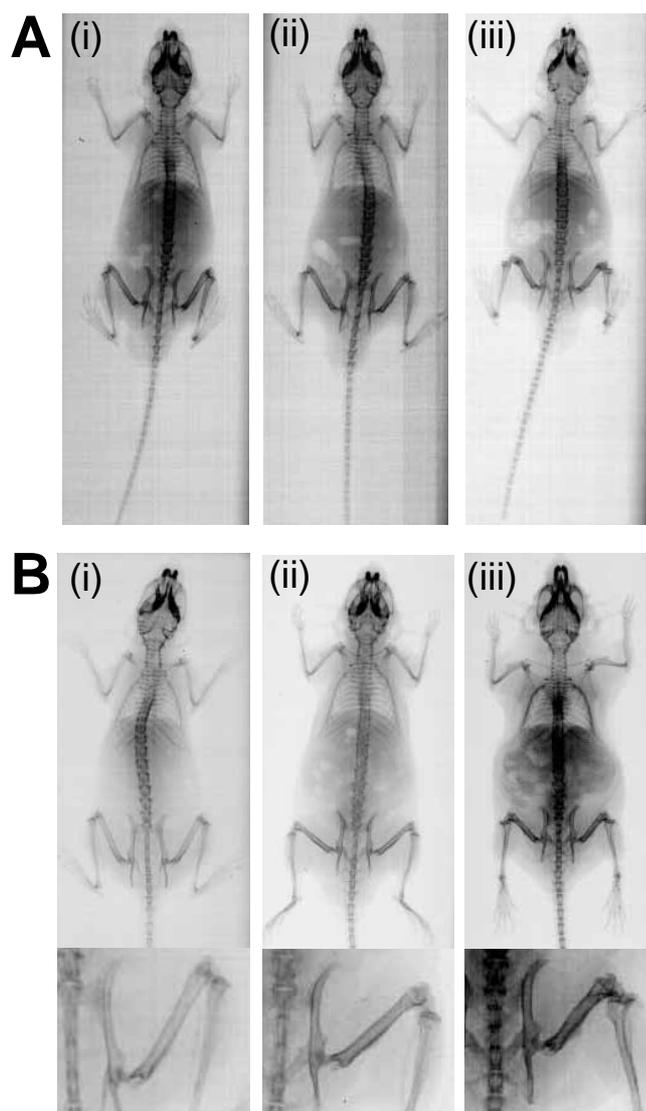

Fig. 2. Skeletal surveys during growth of *Acp 5* mutant mice. Radiographs of homozygous Acp 5 null animals compared with sex-matched littermate controls. (A) Radiographs of (i) wild-type, (ii) heterozygous and (iii) homozygous *Acp 5* male mutant littermate mice taken 8 weeks after birth. Note the widened and foreshortened limb bones and vertebrae in homozygous mutant animals. (B) Radiographs of (i) wild-type, (ii) heterozygous and (iii) homozygous *Acp 5* male mutant littermate mice taken 28 weeks after birth as follow-up images of the animals depicted in A, above. Note the persistent skeletal abnormalities and increased mineralization with growth failure in the long bones and vertebrae. Magnified views illustrate deformities at the metaphyses in (ii) and (iii), where skeletal remodelling is normally active.

of BSE signal levels between $C_{22}H_{25}0_{10}Br$ and $C_{22}H_{22}0_{10}Br_4$ (Boyde et al., 1995b).

Osteoclast resorption assay

To measure the activity of isolated osteoclasts in vitro, the volume and area of resorptive pits were measured by confocal laser reflection microscopy after seeding freshly prepared bone cells on to dentine slices (Boyde and Jones, 1985, 1995).

Long bones were removed from freshly killed 2- to 4-day-old 129 congenic strain mice of defined *Acp 5* genotype and the washed,

pared shafts were diced in Eagle's minimum essential medium containing 10% ^{v}/v fetal calf serum and 2 mM L-glutamine. The bone cells were released by gentle pipetting and aliquots of the suspension were seeded onto 5×5×0.2 mm slices of sperm whale dentine (sterilized by drying from absolute ethanol). After settling for 1 hour, the non-adherent cells were washed off and fresh medium was added for further culture at 37°C in an atmosphere of 5% CO_2 for 28 hours. The slices were then cleaned of cells with detergent containing 4% ^{w}/v chlorhexidine gluconate, washed in water and stained with 1% ^{w}/v toluidine blue in 1% ^{w}/v sodium tetraborate to enhance the identification of resorption pits (Boyde and Jones, 1985).

Measurement of resorption pits was carried out as described using a video-rate, line-confocal reflection light microscope ILM2W (Lasertech Corporation, Japan; Boyde and Jones, 1995). Dentine specimens were coded randomly before counting of the pits to exclude bias. A 40×0.95 NA dry objective, with a coverslip correction and coverslip cemented to the objective was used. The volume below the surface and the area were returned by dedicated software (SIS, Münster, Germany) and mean depth calculated as volume/area for each pit. Non-parametric data analysis was carried out using Minitab statistical software.

Table 1. Type 5 acid phosphatase activity in mutant mice

Acp 5 genotype	Enzyme activity (μmol 4-nitrophenol/min/femur)†
+/+	0.748±0.086 (6)
+/−	0.450±0.057 (8)
−/−	<0.001* (6)

*Undetectable in all samples.
†Mean values with standard errors; number of mice in parentheses.

RESULTS

Targeted disruption of the murine *Acp 5* gene creates a null mutation.

The targeting replacement vector, Acp 5(neo)tk (Fig. 1A), was used to disrupt exon 2 of the single *Acp 5* gene that maps to mouse chromosome 9 (Grimes et al., 1993) in a region that is syntenic with human chromosome 19p22, to which the single human *Acp 5* locus maps (Lord et al., 1990). This exon
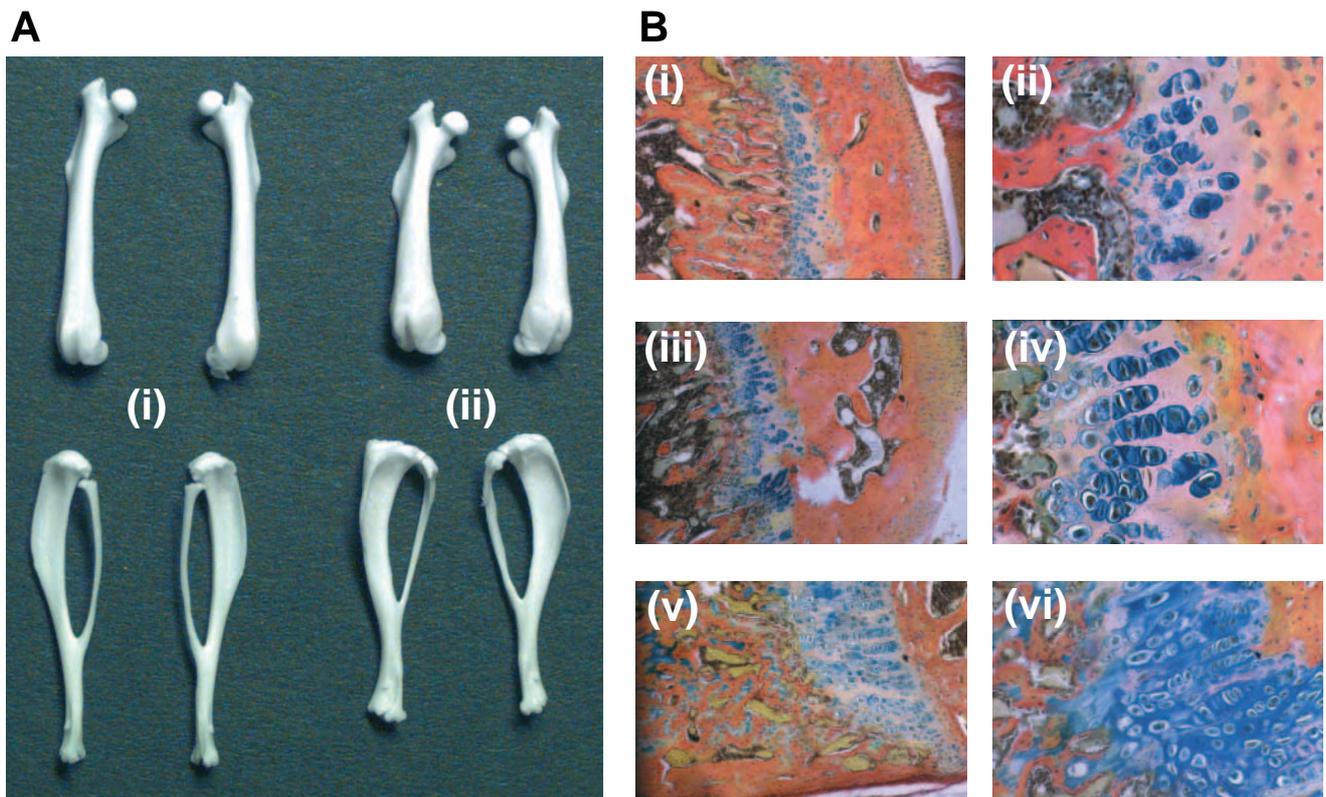

Fig. 3. Structure of cartilaginous growth plates in mutant animals. (A) Hind-limb bones from (i) wild-type and (ii) homozygous mutant 129 strain congenic mice aged 7 months. Bones were dissected free of soft tissues and measured with fine calipers before heating to 95°C in 0.9% ^{w}/v NaCl for 2 hours. Crude papain powder (Sigma Chemical Co. MD) was added to 100 mg/ml and the tissues incubated for 48 hours at 38°C. After repeated rinsing in water, the bones were exposed to 3% ^{w}/v H_2O_2 for 2 hours and the bleached products were finally delipidated in anhydrous acetone before drying. Note the shortening, widening and conical remodelling deformities of bones from Acp 5 −/− mice. (B) Alcian blue-picrofuchsin stained sections of distal femurs from (i, ii) wild-type, (iii, iv) heterozygous and (v,vi) homozygous Acp 5 mutant animals, killed at age 10 weeks. Magnification: (i,iii,v) ×100; (ii,iv) ×400 and (vi) ×200. Note expanded and disorganized epiphyseal plate in homozygous mutant mice compared with heterozygous and wild-type littermate controls. The mucopolysaccharide components of chondrocytes in the cartilaginous zone stain metachromatically with alcian blue. The hyperplastic chondrocyte columns in the mice lacking Acp 5 are disordered and extend into the region where trabecular bone is formed in the zone of secondary ossification. Note the increased size of the chondrocytes especially in the Acp 5 −/− sample, which is shown at medium rather than high magnification in (vi) to take account of the greatly widened growth plate.

contains the putative iron-binding domains of the protein (Lord et al., 1990) and its replacement by homologous recombination is predicted to create a null mutation. Of 14 G418 and GANC double-resistant embryonic stem (ES) cell clones examined by Southern blot analysis, four had undergone the correct targeting event (Fig. 1B) and cells derived from two were injected into C57BL/6 blastocysts. Germ-line transmission was obtained from both ES clones and Southern blot analysis indicated that about half the agouti offspring were heterozygous for the targeted mutation, *Acp 5* +/−, (Fig. 1C). These were intercrossed to obtain animals homozygous for the mutation (*Acp 5* −/−) (Fig. 1D).

Viable fertile homozygous mutant mice were obtained at a frequency indicating that an intact *Acp 5* locus is neither required for gamete formation nor for embryonic development i.e. 22 out of 92 progeny (11 male 11 female). Amplification across exon 2 of the murine *Acp 5* gene using the polymerase chain reaction detected the presence of wild-type sequence only in animals heterozygous or wild type at this locus, and not in *Acp 5* −/− mice. The disrupted *Acp 5* locus showed a structure that was entirely consistent with the predicted homologous replacement event.

That the engineered disruption of the *Acp 5* gene inactivated osteoclast tartrate-resistant acid phosphatase in the *Acp 5* −/− mice was confirmed by assaying acidified detergent extracts of whole bone (Table 1). Because these extracts may also contain the genetically distinct red cell isoform of tartrate-resistant acid phosphatase (Acp 1) present in haematopoietic bone marrow (Frezal et al., 1991), an immunoenzymatic assay selective for the band 5 isozyme of acid phosphatase was used (Echetebu et al., 1987). No acid phosphatase activity attributable to the band 5 isozyme was detected in the bone extracts of *Acp 5* −/− mice. The absence of acid phosphatase activity specifi-

cally from osteoclasts of *Acp 5* −/− mice was confirmed by isolating adherent multinucleated osteoclasts freshly from the long bones of *Acp 5* +/+ and −/− animals and staining for acid phosphatase activity histochemically using the Naphthol/diazonium procedure incubated at pH 5.0 (Burstone, 1958).

Phenotype of *Acp 5* −/− mice

Under laboratory conditions, homozygous mutant mice remain healthy for at least 18 months and seemingly show normal somatic development and reproductive capacity. They behave as expected and appear to hear normally on startling.

Radiographic examination of the homozygous mutant animals (Fig. 2) consistently showed skeletal deformities, with widening and foreshortening of the long bones, most evident
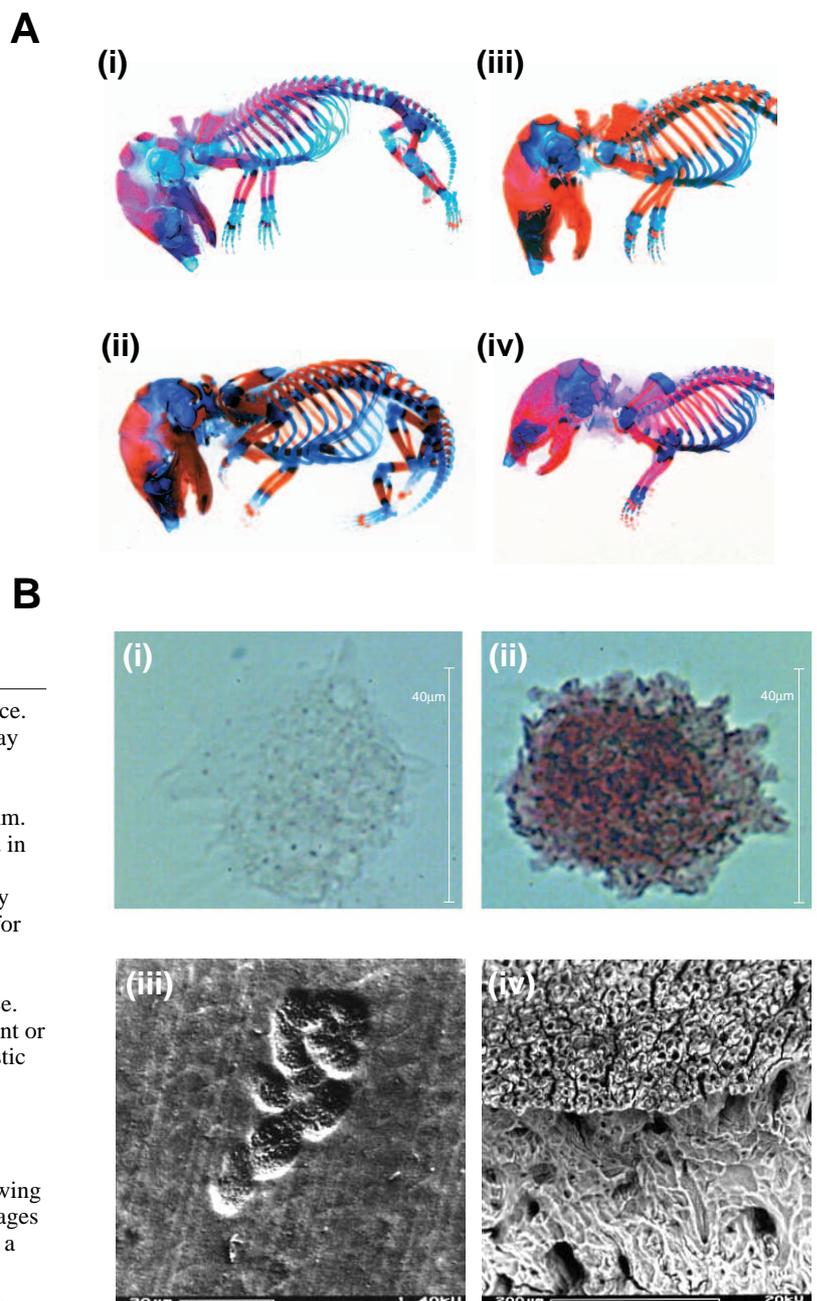
Fig. 4. (A) Skeletal structure in embryonic and newborn mice. Alizarin Red- and Alcian Blue-stained preparations of 18 day embryos ((i), wild type; (ii), Acp 5 mutant) and 1-day-old neonatal animals (iii) wild type; (iv) Acp 5 mutant) are depicted. The crown–rump length of the embryos was 17 mm. After removing the skin and viscera, the animals were fixed in 95% ᵛ/v ethanol before staining in ethanolic Alcian Blue (Sigma) acidified with glacial acetic acid. After rinsing, they were counterstained with caustic Alizarin Red and cleared for storage in 2% KOH glycerol as described by Hogan et al. (1994). Cartilage stains blue and bone is stained red.
(B) Osteoclasts and resorption of bone in Acp 5 mutant mice. Osteoclasts were isolated from freshly killed (i) *Acp 5* mutant or (ii) wild-type, 10 day-old mice and allowed to settle on plastic dishes before staining for acid phosphatase activity by the Naphthol/diazonium procedure at pH 5.0. (iii) Scanning electron microscopy of resorption pits obtained by seeding osteoclasts from femurs of 4 day-old *Acp 5* −/− mice onto polished dentine is depicted after washing the surface following culture in vitro for 28 hours. (iv) Backscattered electron images of the calcified zone of cartilage in the epiphyseal region of a vertebra from a homozygous *Acp 5* null mouse showing resorption lacunae resulting from osteoclast activity in vivo.

in the humeri, vertebrae and femora. Direct measurement of the lengths of freshly removed femurs from congenic 129 strain mice demonstrated reduced bone growth in homozygous mutants: at four weeks, mean femoral length in six was 4.68±0.05 (s.d.) mm, compared with 4.98±0.08 (s.d.) mm in six wild-type controls, ($P<0.001$). In adults aged 4-7 months, however, mean femoral lengths in ten $Acp\ 5$ −/− mice were 5.59±0.02 (s.d.) mm, compared with 6.44±0.27 mm in twelve +/+ controls, ($P<0.0001$). A distinct club-like deformity was observed in the distal femora and was associated with pyramidal malformation of the proximal tibiae, this appeared to increase with age (Fig. 3A). Abnormalities of the axial skeleton were also observed in Acp 5-deficient mice, with shortened vertebrae especially in the caudal region.

The skeletal defects were observed in homozygous mutant mice at 8 weeks of age but the foreshortening of long bones and modelling deformities became more apparent later with the development of increased mineralized bone density (see below). Intermediate changes in the skeleton were observed in older heterozygotes ($Acp\ 5$ +/−) mice. No sex differences in the mutant phenotype were seen and haemoglobin concentrations and peripheral blood cell counts of the mutant animals remained within the range of their unaffected age-matched controls indicating that the marrow space was not significantly occluded.

Microscopical examination of bone sections (Fig. 3B) showed expansion of the cartilaginous growth plates with disruption of the ordered arrangement of chondrocytes during differentiation in the homozygous $Acp\ 5$ mutant mice. The chondrocytes showed marked hypertrophy and hyperplasia with increased retention of thicker metaphyseal trabeculae associated with reduced modelling and mineralization of the expanded cartilaginous matrix. Von Kossa staining of undecalcified sections, however, confirmed that there were no differences in the width and structure of mineralized osteoid seams (not shown), as would have been expected in rachitic bone. Multinucleated osteoclasts were readily identified on haematoxylin-eosin-stained sections (not shown), and in wild-type ($Acp\ 5$ +/+) bone stained strongly for tartrate-resistant acid phosphatase. In homozygous mutant mice, abundant osteoclasts had invaded the epiphyseal growth plates within the disorganized region of modelling and ossification, indicating a qualitative defect of cell function. Formation and development of membrane bones in the skull, auditory ossicles and clavicles as well as tooth eruption appeared to be normal in lateral skull radiographs (not shown) and in alizarin-stained skeletal preparations obtained from embryonic animals and during the first days of life of (Fig. 4A) Acp 5-deficient mice. However, BSE image analysis revealed increased bone mineralization density (see below). Absence of osteoclast-specific acid phosphatase activity was confirmed by staining freshly isolated multinucleated cells (obtained from homogenized long bones of wild-type and homozygous mutants) that were allowed to settle on plastic surfaces or to resorb sections of dentine where the pits were imaged by scanning electron microscopy (Fig. 4B). The presence of osteoclastic resorption lacunae *in vivo* in all specimens was confirmed (Fig. 4B). Although the gross morphology of the endoskeletal bones differed, the morphology of the mineral front preparations was similar in bones from animals of all three genotypes (Fig. 5).

Effects on endochondral bone formation

To define further the skeletal effects of deficiency of osteoclastic acid phosphatase caused by the null $Acp\ 5$ mutation, we analysed polymethylmethacrylate (PMMA)-embedded mouse bones by digital imaging using BSE-SEM (Boyde et al., 1995a,b).

This procedure provides whole bone images of the mineralized tissues and permits quantification of the mineralization abnormalities in the mutant mice. Examination of tail vertebrae from littermate animals aged eight weeks confirmed that the $Acp\ 5$ −/− mice had wider, shorter bones with thickened cortices and disorganised, as well as expanded, growth plates (Fig. 5). The metaphyseal trabecular bone was thickened in both the heterozygous $Acp\ 5$ +/− and homozygous mutants (−/−) compared with wild-type control animals; the growth plates, however, were only clearly abnormal in the homozygous mutants. At this age, the bones of the homozygous mutant ($Acp\ 5$ −/−) mice were less well mineralized in the diaphyseal region than in the heterozygous (+/−) and wild-type (+/+) controls. The appearances of the mineralizing cartilage and the overall bone mineral content indicate that endochondral ossification is impaired as a result of a mineralization defect in the mice completely lacking osteoclastic acid phosphatase. This conclusion is supported by the presence of a wider zone within which microcalcospherites remain distinguishable in the calcified cartilage in the homozygous mutants, (Fig. 5C-E). High magnification views of the region of resorption of calcified cartilage show abundant osteoclastic lacunae in the samples obtained from animals of each genotype.

Effects on skeletal mineralization

Serial studies of live mice suggested progressive increases in bone radiographic density in $Acp\ 5$ mutant mice; these represent changes in total bone mineral mass per unit cross section with age (Fig. 2A,B). Subsequent BSE analysis of bone samples obtained from congenic 129 strain mice of defined $Acp\ 5$ genotype confirmed that overall bone mineralization density was increased in $Acp\ 5$ null (−/−) and heterozygous ($Acp\ 5$ +/−) animals. These changes were identified in membrane bones (mandibles and calvaria) as well as in the shortened and deformed endochondral bones.

By 12 weeks of age, epiphyseal bone in the −/− homozygotes and heterozygous animals was thicker and more highly mineralized than in the wild-type mice (Fig. 6). These changes were associated with a greater proportion of bone in epiphysis and metaphysis despite the persistence of widened growth plates (restricted to the homozygous −/− animals) and reduced growth (Fig. 5F,G). Quantitative image analysis from the three distinct regions (epiphysis, metaphysis and diaphysis) of vertebrae and femurs showed significantly increased mineralization density in all regions of the mutant (−/−) and heterozygous (+/−) age-and sex-matched animals compared with wild-type controls (Figs 6, 7). These findings contrast markedly with the analysis of the same bones in the eight-week old mice, where during bone formation and growth, there was a slight *decrease* in mineralized tissue in the (−/−) animals) (Fig. 6A).

BSE image analysis of calvarial bones from young (7 days) and older animals (3, 6, 7 and 13 months) showed increased mineralization of sections obtained from $Acp\ 5$ −/− samples (see Fig. 7). Multiple sections were obtained from at least two
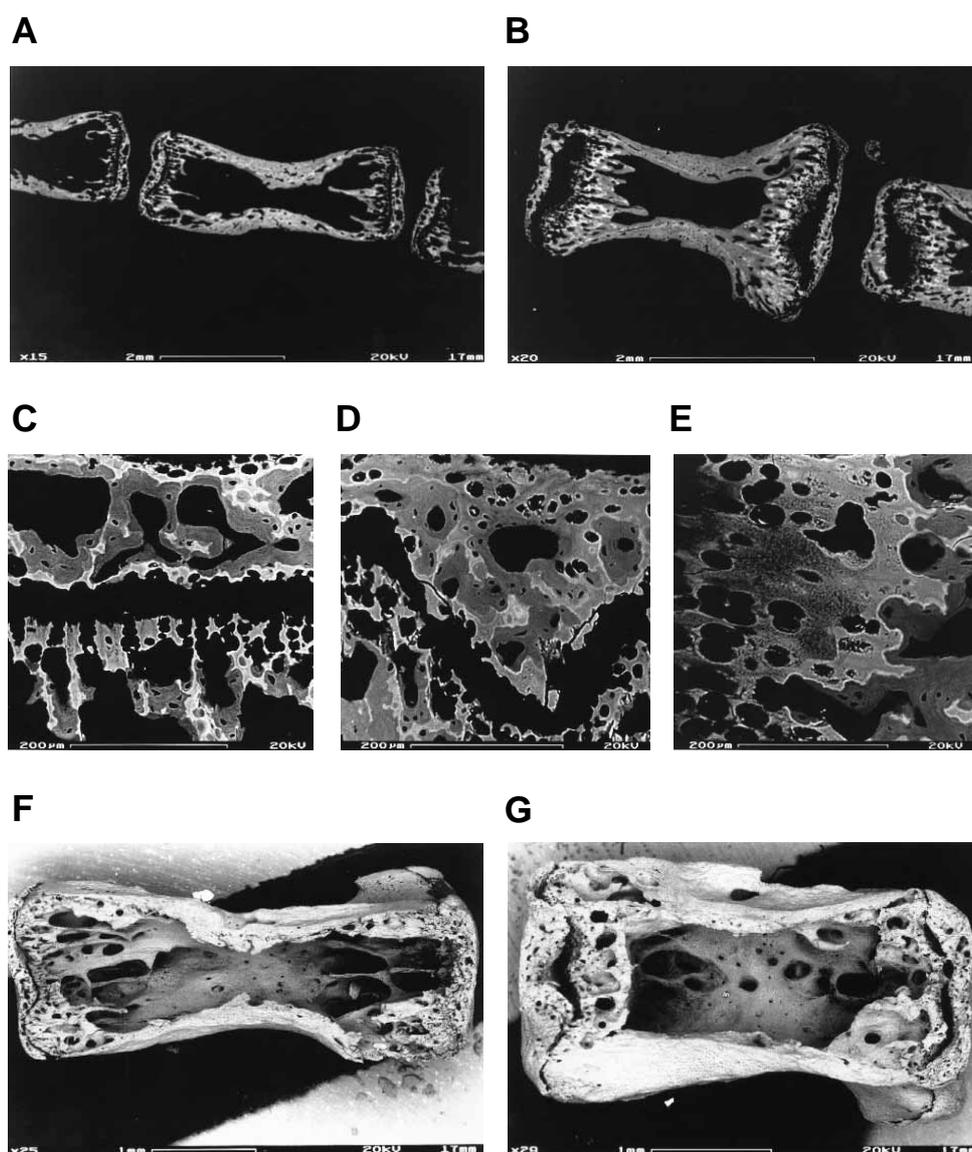
Fig. 5. Microscopic structure of individual bones from *Acp 5* mutant mice. Low- (A,B) and high-magnification (C,D,E) BSE images obtained from tail vertebrae of 2-month-old animals. (A,C) Wild-type, (D) heterozygous *Acp 5* +/− and (B,E) homozygous *Acp 5* −/− mice. Calcified cartilage is recognized in these images as the whitest phase: the unmineralized part of the growth plate and other non-mineralized tissue appear black. Note the widened disorganized growth plates in the mutant animals, without stacked columns of chondroblasts; the bones are overall fatter, shorter and have thicker cortices than vertebrae from wild-type and heterozygous animals. Scanning electron micrographs of three-dimensional surfaces of tail vertebrae from 3 month-old (F) wild-type and (G) homozygous *Acp 5* null mice made anorganic by exposure to sodium hypochlorite. After washing, the bones were dehydrated with ethanol, air dried and carbon coated by evaporation. Note the reduced size of the bone from the mutant animals, its abnormal shape with altered trabecular sculpting at the metaphyses and widened growth plate spaces. The thickened subchondral bone on the metaphyseal side of the growth plates provides evidence that osteopetrosis has already become established.

animals in each group matched for age and sex. At each age studied, mineralization density increased and was significantly greater ($P<0.013$) in Acp 5 −/− calvaria compared with Acp 5 +/+ even at 13 months of age (not shown).

The densities of dentine and of the erupted, mature enamel were not distinguishable in the three groups of mice (not shown).

Thus mice deficient in acid phosphatase activity in osteoclasts (either homozygotes (−/−) or heterozygotes (+/−)) develop a mild osteopetrosis with increased bone tissue, which is more highly mineralized than in control, wild-type animals. These features suggest that bone resorptive activity by acid phosphatase-deficient osteoclasts in vivo, though present, is qualitatively impaired.

Effects on osteoclastic resorption of mature bone

The presence of resorption lacunae in the ossification zones of calcified cartilage together with the normal dentition of *Acp 5* −/− mice, demonstrates that osteoclasts are present during endochondral ossification in long bones. However, the devel-

opment of pyramidal modelling deformities and generalized increases in skeletal mineralization in older animals (and even at 7 days in calvarial sections) suggest that the homozygous *Acp 5* mutant and heterozygous mice have a qualitative defect of osteoclastic activity leading to an imbalance between new bone formation and resorption.

Effects on osteoclast resorption activity in vitro

To measure resorptive activity, fresh osteoclasts were isolated from the shafts of the long bones of mice 2-4 days old and seeded as a suspension on to dentine sections (Boyde and Jones, 1985). The resorption pits were stained and the specimens coded randomly before imaging by transmitted light microscopy; mean pit depth was estimated by calculating the ratio of volume to area determined by confocal reflection microscopic mapping (Table 2).

As shown in Fig. 4, osteoclasts lacking tartrate-resistant acid phosphatase activity were readily isolated from *Acp 5* −/− mice and were capable of adhering to the surface of the mineralized matrix to form resorptive foci.
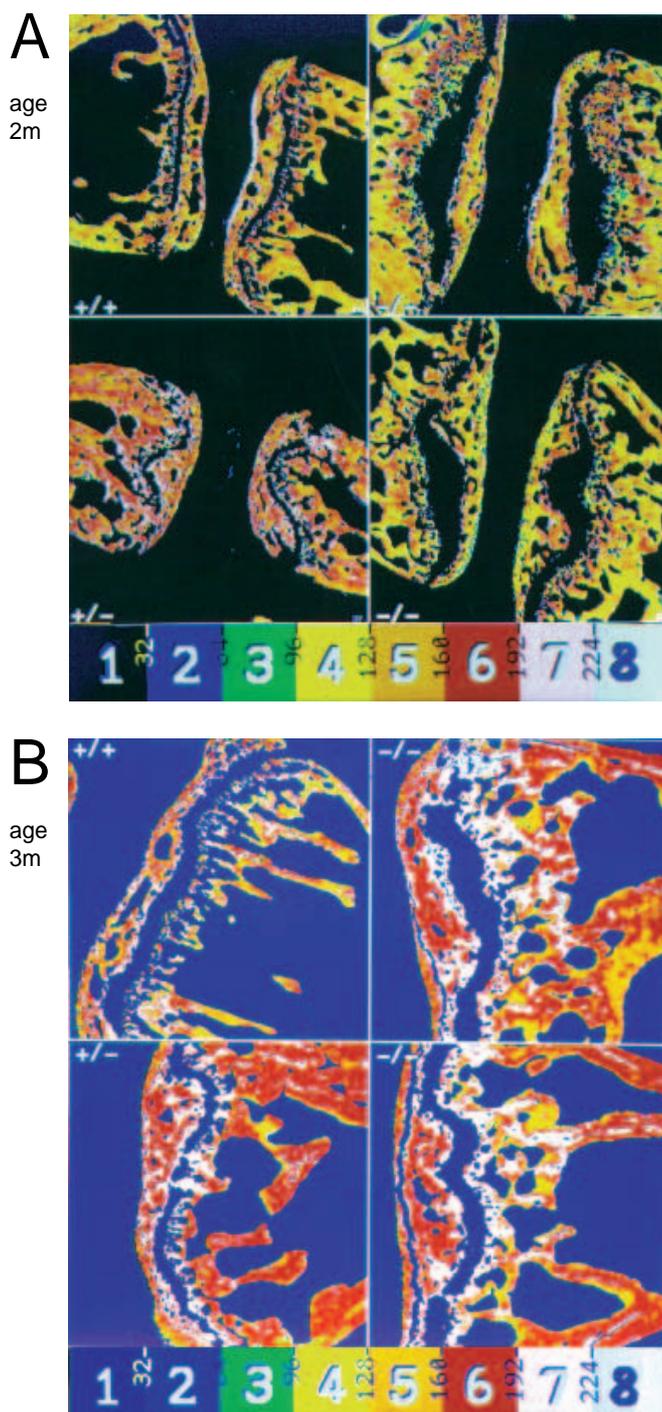
Fig. 6. Evolution of bone structure and mineral density in *Acp 5* mutant mice. Colour-coded BSE images obtained in epiphyseal and metaphyseal regions of tail vertebrae from congenic animals of indicated genotype aged: (A) 2 months and (B) 3 months. Here the mineralization densities have been surveyed over a close stereological grid with non-overlapping sampling points: the signal levels at each point have been coded into one of eight density ranges represented in contrasting colours as shown on the colour scale strips. Note the altered mineralization density as well as the altered trabecular structure in the *Acp 5* −/−and the +/− animals, compared with the wild type (+/+). These changes are accentuated rapidly during maturation and indicate reduced resorption activity.
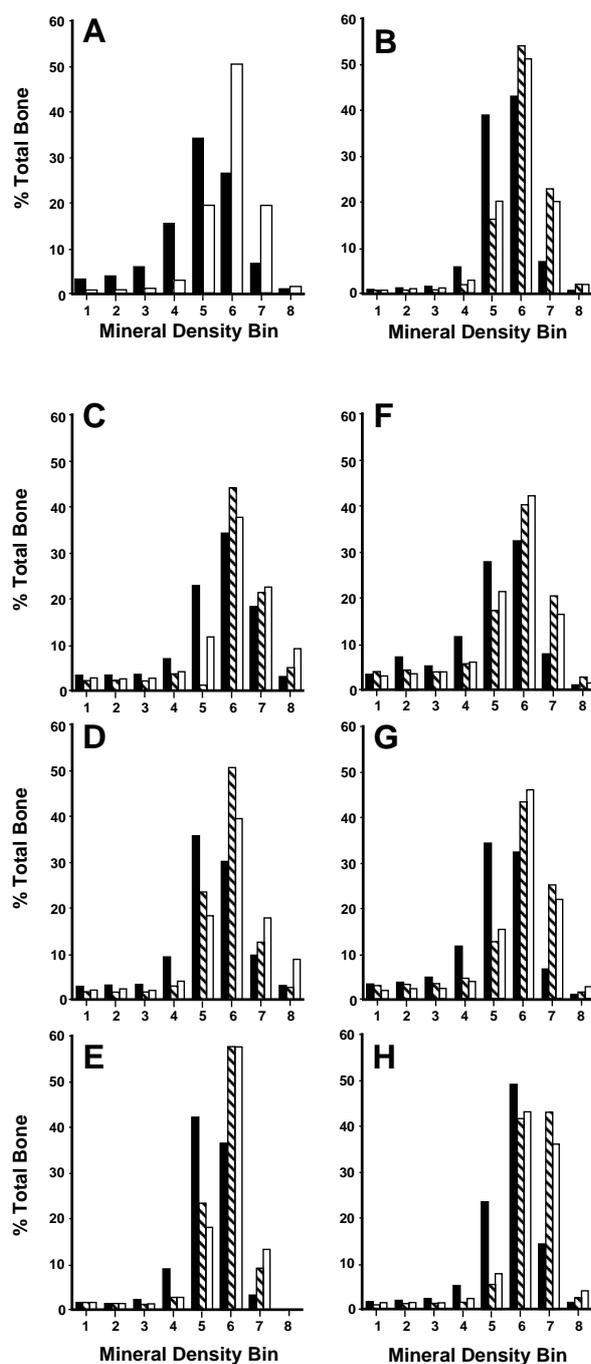

Fig. 7. Quantitative skeletal histomorphometry. Measurement of bone mineralization density in *Acp 5* mutant mice at different ages. These data are represented as histograms obtained from the BSE analysis using the same eight bin categories depicted in Fig. 6. (A,B) Calvarial sections obtained from congenic strain mice aged 7 days and 3 months, respectively, to show representative changes in mineralization density observed in membrane bone samples from mice up to 13 months of age. (C-E) Respectively epiphyseal, metaphyseal and diaphyseal regions of femurs; (F-H) epiphyseal, metaphyseal and diaphyseal regions of tail vertebrae respectively. Bars represent mean data from 2-8 fields for each region of bones from: solid bars, wild-type mice; hatched bars, samples from mice of +/− genotype and open bars, samples from homozygous mutants. The distribution of mineralized bone is displaced in all regions of both types of bone sampled in heterozygous and *Acp 5* null mice ($P \leq 0.013$).

Table 2. Resorption of dentine by mouse osteoclasts in vitro

Acp 5 genotype	No. of pits	Pit volume (μm^3)	Pit area (μm^2)	Mean depth (μm)
+/+	595	3115±193	990±52.1	2.61±0.04
−/−	450	2385±190*	880±64.0*	2.44±0.05*

Values are shown as mean and standard error

*$P<0.0001$ (determined by the non-parametric rank order Mann-Whitney Test adjusted for ties).

However osteoclastic resorption activity, as determined by the pit assay procedure, was impaired in cells obtained from *Acp 5* null mice when compared with those from congenic 129 strain wild-type animals. It is noteworthy that all parameters of osteoclasis in vitro were significantly reduced in the Acp 5-deficient mice (Table 2).

DISCUSSION

Development of the skeleton involves the growth, shaping of bones (modelling) and coupled formation and resorption of osseous mineral and matrix by osteoclasts (remodelling). Acp 5-deficient mice show impairment of all three processes. Endochondral growth requires the orderly proliferation, maturation and degeneration of chondrocytes that originate from the epiphyseal plate. Calcification of the cartilaginous matrix occurs in association with membrane-bound extracellular vesicles – matrix vesicles – that contain abundant alkaline phosphatase activity (Ali, 1986; Majeska and Wuthier, 1975). Mineralization is associated with the appearance of crystals within these vesicles, which ultimately rupture to allow extracellular crystal growth.

Although ossifying cartilage and bone have long been known to contain abundant alkaline phosphatase activity in osteoblasts that may raise phosphate concentrations locally to allow mineralization (Robison, 1923), it has been more recently suggested that this enzyme promotes mineralization by hydrolyzing pyrophosphate, itself an inhibitor of mineralization (Fleisch et al., 1966; Moss et al., 1967). Support for this proposal has emerged from studies of human non-specific alkaline phosphatase deficiency (Whyte, 1995). Humans with reduced alkaline phosphatase activity have defects of skeletal mineralization and dental abnormalities with elevated concentrations of plasma pyrophosphate: the natural substrate for alkaline phosphatase in bone is, however, unknown.

We have identified radiological and microscopic abnormalities of bone and cartilage in *Acp 5* homozygous mutant mice that suggest a contributory rôle for this osteoclastic enzyme in the mineralization of extracellular cartilage matrix during bone growth. Widened zones of hypertrophic cartilage with disorganization of the proliferating chondrocytes in the epiphyseal growth plate of the homozygous mutants resemble the rachitic changes in infants and children with severe non-specific alkaline phosphatase deficiency (Ornoy et al., 1985). It is noteworthy, however, that gene knockout mice lacking the nonspecific alkaline phosphatase have apparently normal growth plates but develop deformities in the long bones by six months of age (Waymire et al., 1995).

The matrix of cartilage and bone is rich in phosphoproteins such as osteopontin and bone sialoprotein that contain the RGD motif, which interacts with the vitronectin receptor, $a_v\beta_3$ integrin (Oldberg et al.,1986). Although bone sialoprotein binds calcium and hydroxyapatite (Chen et al., 1992), osteopontin, which is selectively deposited at the mineralization front (Hultenby et al., 1994), appears to inhibit hydroxyapatite formation (Boskey et al., 1993; McKee and Nanci, 1996). There is thus an abundance of potential substrates for phosphatases in bone and the recent finding that osteoclasts as well as osteoblasts may also secrete regulatory phosphoproteins such as osteopontin (Dodds et al., 1995) indicates that these cells may contribute to mineralization as well as resorption of calcified matrix during modelling/remodelling. Evidence that phosphotyrosine protein phosphatase activity conditions skeletal matrix for ossification (Lau et al., 1985); that *Acp 5* is a powerful catalyst of phosphotyrosyl peptide hydrolysis (Nash et al., 1993); and that *Acp 5* can dephosphorylate osteopontin and bone sialoprotein, which are resistant to alkaline phosphatase (Ek-Rylander et al., 1994), specifically implicates osteoclastic acid phosphatase in the mineralization pathway. Since, unlike their parent proteins, dephosphorylated osteopontin and bone sialoprotein can no longer promote attachment of osteoclasts (Ek Rylander et al., 1994), acid phosphatase activity may regulate recruitment of osteoclasts to the mineralization front.

The maturing axial skeletons of *Acp 5*-deficient mice show persistent deformities associated with reduced modelling and remodelling activity by osteoclasts. Unlike animals before the age of two months, three-month-old and older mice lacking *Acp 5* show increased mineralization density in all bone regions with thickened trabeculae. These biphasic effects were unexpected. That similar changes were observed in the bones of older heterozygous *Acp 5* +/− animals, indicates that the protein has a critical function in the maintenance of skeletal integrity in adult bone for which the threshold effect of its deficiency cannot be compensated. Finally, progressive increases in the mineralization of the membrane bones of the skull, which appear to develop normally in *Acp 5*-deficient mice, are manifestations of reduced bone turnover by osteoclasts with a resorptive defect. This points to a quantitative control by the *Acp 5* gene product that is exerted on osteoclast function. The nature of the deformity of long bones and remodelling defect in *Acp 5*-deficient mice shows that reduced expression of the *Acp 5* gene product impairs, but does not abolish, osteoclastic resorption.

Acp 5 deficiency represents a mild form of murine osteopetrosis that is shown by the increased bone mineralization density and unequivocal thickening of the subchondral bone plates (Figs 5, 6). The skeletal phenotype shares several features with other murine osteopetrotic mutants (Marks and Walker, 1976) but it is less severe. A notable feature of the *Acp 5* mutants is their normal dentition, indicating that resorption of mandibular bone is sufficiently active to allow growth and eruption of the teeth, a process that is delayed or absent in the more severe osteopetrotic mutants.

The spontaneous *op* mutant is caused by deficiency of colony-stimulating factor-1 (CSF-1) and leads to reduced formation of osteoclasts and macrophages from myeloid progenitor cells (Wiktor-Jedrzejczak, 1990). Targeted disruption of the murine *Src* and *Fos* proto-oncogenes is associated with recessive variants of severe osteopetrosis (Soriano et al., 1991;

Johnson et al., 1992) due to defects in osteoclast function and differentiation, respectively (Lowe et al., 1993; Grigoriadis et al., 1994, 1995). It is noteworthy that, as in c-src deficient mice, the abnormal metaphyseal regions of bone in *Acp 5* mutant mice contain abundant osteoclasts with impaired function. This conclusion is supported by the results of the pit assay determinations of osteoclastic resorption activity in vitro. Although the spontaneous formation of heterokaryons may affect pit size and apparent resorptive activity of osteoclasts (Piper et al., 1992), significant decreases in all parameters, including mean depth measured in a large number of pits, would discount variation due to cell size differences in the homozygous mutants. Thus the comparisons between normal and *Acp 5*-deficient osteoclasts indicate that they have cell-intrinsic defects of resorptive activity.

In contrast to c-src or Acp 5-deficient mice, CSF-1-deficient osteopetrotic mice have markedly reduced numbers of osteoclasts and macrophages because expansion and differentiation of their myeloid precursors fails to occur in the bone marrow. Recent experiments have shown that neither marrow transplantation nor administration of purified CSF-1 completely restores the remodeling defect in neonatal *op/op* mice, even though osteoclast numbers return to normal (Sundquist et al., 1995). Thus local factors that influence the migration of osteoclasts and macrophages to the sites of resorption at the metaphyses are required to reverse this defect.

Mice lacking the *Fos* nuclear proto-oncogene have a selective arrest in the differentiation of myeloid progenitors into cells of osteoclast lineage: in the absence of multinucleated osteoclasts, the skeletal defect typical of osteopetrosis occurs despite the recruitment of more bone marrow macrophages (Grigoriadis et al., 1994). The skeletal phenotype of *Fos* mutant mice was rescued both by marrow transplantation and by ectopic c-Fos expression which overcomes the differentation arrest. Thus selective absence of functional osteoclasts impairs formation of bone specifically at sites of active remodelling. Our studies point to a partial defect of intrinsic osteoclast function in mice that lack osteoclastic acid phosphatase. In heterozygous *Acp 5* +/− mice, a threshold effect is evident.

Osteoclasts resorb the skeleton by degrading matrix and mineral; recent data suggest that they may also synthesise bone matrix proteins, which they can modify and to which they may later adhere (Dodds et al., 1995). Type 5 acid phosphatase dephosphorylates bone matrix proteins (Ek-Rylander et al., 1995) but, because it is also an iron protein with electrochemical properties, it may also degrade matrix by promoting formation of free radicals (Hayman and Cox, 1994). The presence of a unique Fe^{2+}/Fe^{3+} cluster in the purple phosphatases, of which *Acp 5* is a member, allows the generation of hydroxyl free radicals by means of Fenton chemistry (Sibille et al., 1987; Hayman and Cox, 1994). Reactive oxygen species including superoxide, are produced at the ruffled border of the osteoclast during bone resorption (Garrett et al., 1990; Key et al., 1994; Steinbeck et al., 1994). Co-secretion of type 5 acid phosphatase into the resorptive vacuole at the bone interface further implicates this protein in the augmentation of matrix-degrading functions of the osteoclast, and we have suggested that it may serve to enhance the formation of highly reactive radical species from superoxide and nitric oxide (Hayman and Cox, 1994).

The disordered ossification and growth of endochondral bones in *Acp 5*-deficient mice reported here indicates an unsuspected function for this protein. The disorganization of the growth plate in the mutants resembles that reported recently in chondrodysplastic mice generated by targeted disruption of the activating transcription factor-2 (ATF-2) gene (Reimold et al., 1996). ATF-2 binding sites have been identified in the promoter regions of genes involved in skeletal development, including osteopontin, osteocalcin and alkaline phosphatase.

The osteopetrosis observed in Acp 5 −/− mice is definite but mild. The resorption defect allows tooth eruption to occur and the diploic and marrow spaces are not significantly encroached upon, so that the Acp 5 −/− skeleton does not manifest the florid changes observed in human Albers-Schönberg disease or the other severe defects observed in experimental osteopetrotic animals. Nonetheless, the resorption defect affects skeletal modelling and remodelling and bone mineralization density is unequivocally increased as a result of reduced turnover. Osteoclastic acid phosphatase could be a target for the therapy of metabolic diseases of adult human bone, including osteoporosis. The *Acp 5* mutant mouse provides an experimental model for analysing cartilage and bone development; it should also prove informative in combination with other genetic defects of the skeleton.

REFERENCES

Ali, S. Y. (1986) *Cell Mediated Calcification and Matrix Vesicles.* New York: Elsevier.

Boskey, A. L., Maresca, M., Ullrich, W., Doty, S. B., Butler, W. T. and Prince, C. W. (1993). Osteopontin-hydroxyapatite interactions in vitro: inhibition of hydroxyapatite formation and growth in a gelatin-gel. *Bone Miner.* **22**, 147-159.

Boyde, A. and Jones, S. A. (1985) Optical and scanning electron microscopy in the single osteoclast resorption assay. *Scann. Electron. Micros.* **1985/III**, 1259-1271.

Boyde, A., Jones, S. J., Aerssens, J. and Dequeker, J. (1995a). Mineral density quantification of the human cortical iliac crest by backscattered electron image analysis: variations with age, sex and degree of osteoarthritis. *Bone* **16**, 619-627.

Boyde, A., Davy, K. W. M. and Jones, S. J. (1995b). Standards for mineral quantitation of human bone by analysis of backscattered electron images. *Scanning* **17**, Suppl. v: 6-7.

Boyde, A. and Jones, S. J. (1995). Mapping and measuring surfaces using reflection confocal microscopy. In *Handbook of Biological Confocal Microscopy.* (ed J. B. Pawley). 2nd Edition. pp. 255-266. New York: Plenum Press.

Burstone, M. S. (1958). Histochemical comparison of naphthol As-phosphates for the demonstration of phosphatases. *J. Natl. Cancer Inst.* **21**, 523-538.

Cassady, A. I., King, A. G., Cross, N. C. P. and Hume, D. A. (1993). Isolation and characterization of the genes encoding mouse and human type-5 acid phosphatase. *Gene* **130**, 201-207.

Chamberlain, P., Compston, J., Cox, T. M., Hayman, A. R., Imrie, R. C.,

Reynolds, K. and Holmes, S. D. (1995). Generation and characterization of monoclonal antibodies to human type-5 tartrate-resistant acid phosphatase: development of a specific immunoassay of the isoenzyme in serum. *Clin. Chem.* **41**, 1495-1499.

Chen, J., Shapiro, H. S. and Sodek, J. (1992). Developmental expression of bone sialoprotein mRNA in rat mineralized and connective tissues. *J. Bone Miner. Res.* **7**, 987-997.

Dodds, R. A., Connor, J. R., James, I. E., Rykaczewski, E. L., Applebaum, E., Dul, E. and Gowen, M. (1995). Human osteoclasts, not osteoblasts, deposit osteopontin onto resorption surfaces: an in vitro ex vivo study of remodeling bone. *J. Bone. Miner. Res.* **10**, 1666-1680.

Echetebu, Z. O., Cox, T. M. and Moss, D. W. (1987). Antibodies to porcine uteroferrin used in the measurement of human tartrate-resistant acid phosphatase. *Clin. Chem.* **33**, 1832-1836.

Ek-Rylander, B., Flores, M., Wendel, M., Heinegård, D. and Andersson, G. (1994). Dephosphorylation of osteopontin and bone sialoprotein by osteoclastic tartrate-resistant acid phosphatase. Modulation of osteoclast adhesion in vitro. *J. Biol. Chem.* **269**, 14853-14856.

Erlebacher, A., Filvaroff, E. H., Gitelman, S. E. and Derynck, R. (1995). Toward a molecular understanding of skeletal development. *Cell* **80**, 371-378.

Evans, M. (1994) Tissue culture of embryonic stem cells. In *Cell Biology: A Laboratory Handbook* (ed. J. Celis), vol. I, pp 54-67. New York: Academic Press.

Fleisch, H., Russell, R. G. G. and Straumann, F. (1966). Effect of pyrophosphate on hydroxyapatite and its implications in calcium homeostasis. *Nature* **212**, 901-903.

Frézal, J., Baule, M. S. and De Fougerolle, T. (1991) *Genetlas* 2nd Edition, London: John Libbey.

Garrett, I. R., Boyce, B. F., Oreffo, R. O. C., Bonewald, L., Poser, J. and Mundy, G. R. (1990). Oxygen-derived free radicals stimulate osteoclastic bone resorption in rodent bone in vitro and in vivo. *J. Clin. Invest.* **85**, 632-639.

Grigoriadis, A. E., Wang, Z. Q., Cecchini, M. G., Hofstetter, W., Felix, R., Fleisch, H. A. and Wagner, E. F. (1994). c-fos: a key regulator of osteoclast-macrophage lineage determination and bone remodeling. *Science* **266**, 443-448.

Grigoriadis, A. E., Wang, Z-Q. and Wagner, E. F. (1995). Fos and bone cell development: lessons from a nuclear oncogene. *Trends Genet.* **11**, 436-441.

Grimes, R., Reddy, S. V., Leach, R. J., Scarcez, T., Roodman, G. E., Sakaguchi, A. Y., Lalley, P. A. and Windle, J. J. (1993). Assignment of the mouse tartrate-resistant acid phosphatase gene (Acp 5) to chromosome 9. *Genomics* **15**, 421-422.

Hayman, A. R., Warburton, M. J., Pringle, J. A. S., Coles, B. and Chambers, T. J. (1989). Purification and characterization of a tartrate-resistant acid phosphatase from human osteoclastomas. *Biochem. J.* **261**, 601-609.

Hayman, A. R. and Cox, T. M. (1994). Purple acid phosphatase of the human macrophage and osteoclast. Characterization, molecular properties and crystallization of the recombinant di-iron-oxo protein secreted by baculovirus-infected insect cells. *J. Biol. Chem.* **269**, 1294-1300.

Hogan, B., Beddington, R., Constantini F. and Lacy, E. (1994). *Manipulating the Mouse Embryo.* 2nd Edition, , pp 379-380. New York: Cold Spring Harbor Laboratory Press

Hultenby, K., Reinholt, F. P., Norgard, M., Wendel, M., Oldberg, A. and Heinegård, D. (1994). Distribution and synthesis of bone sialoprotein in metaphyseal bone of young rats show a distincly different pattern from that of osteopontin. *Eur. J. Cell Biol.* **63**, 230-239.

Johnson, R. S., Spiegelman, B. and Papaionnou, V. (1992) Pleiotropic effects of a null mutation in the c-fos proto-oncogene. *Cell* **71**, 577-586.

Joterau, F. V. and Le Douarin, N. M. (1978). The developmental relationship between osteocytes and osteoclasts: a study using the quail-chick nuclear marker in endochondral ossification. *Dev. Biol.* **63**, 253-265.

Key, L. L. Jr., Wolf, W. C., Gundberg, C. M. and Ries, W. L. (1994) Superoxide and bone resorption. *Bone* **15**, 431-436.

Lau, K. H., Farley, J. R. and Baylink, D. J. (1985). Phosphotyrosyl-specific protein phosphatase activity of a bovine skeletal acid phosphatase isoenzyme. Comparison with the phosphotyrosyl protein phosphatase activity of skeletal alkaline phosphatase. *J. Biol. Chem.* **260**, 4653-4660.

Lau, K. H., Onishi, T., Wergedal, J. E., Singer, F. R. and Baylink, D. J. (1987). Characterization and assay of tartrate-resistant acid phosphatase activity in serum: potential use to assess bone resorption. *Clin. Chem.* **33**, 458-462.

Li, C. Y., Lam, L. T. and Lam, K. W. (1970). Acid phosphatase isoenzyme in human leukocytes in normal and pathologic conditions. *J. Histochem. Cytochem.* **18**, 473-481.

Lloyd, G. E. (1987). Atomic number and crystallographic contrast images with the SEM: a review of backscattered electron techniques. *Mineralol. Mag.* **51**, 3-19.

Lord, D. K., Cross, N. C. P., Bevilacqua, M. A., Rider, S. H., Gorman, P. A., Groves, A. V., Moss, D. W., Sheer, D. and Cox, T. M. (1990). Type 5 acid phosphatase. Sequence, expression and chromosomal localization of a differentiation-associated protein of the human macrophage. *Eur. J. Biochem.* **189**, 287-293.

Lowe, C., Yoneda, T., Boyce, B. F., Chen, H., Mundy, G. R. and Soriano, P. (1993). Osteopetrosis in Src-deficient mice is due to an autonomous defect of osteoclasts. *Proc. Natl. Acad. Sci. USA* **90**, 4485-4489.

Majeska, R. J. and Wuthier, R. E. (1975). Studies on matrix vesicles isolated from chick epiphyseal cartilage. Association of pyrophosphatase and ATP-ase activities with alkaline phosphatase. *Biochem. Biophys. Acta* **391**, 51-60.

Manolagas, S. C. and Jilka, R. L. (1995). Bone marrow, cytokines and bone remodeling. *N. Engl. J. Med.* **332**, 305-311.

Mansour, S. L., Thomas, K. R. and Capecchi, M. R. (1988) Disruption of the photo-oncogene int-2 in mouse embryo-derived stem cells: a general strategy for targeting mutations to non-selectable genes. *Nature* **336**, 348-352.

Marks, S. E. Jr. and Walker, D. G. (1976). Mammalian osteopetrosis – a model for studying cellular and humoral factors in bone resorption. In *The Biochemistry and Physiology of Bone.* (ed. G. H. Bourne). Volume **4**, pp 277-301. New York: Academic Press.

McKee, M. D. and Nanci, A. (1996). Osteopontin at mineralized tissue interfaces in bone, teeth and osseointegrated implants: ultrastructural distribution and implication for mineralized tissue formation, turnover and repair. *Microscop. Res. Technique* **33**, 141-164.

Minkin, C. (1982). Bone acid phosphatase: tartrate-resistant acid phosphatase as a marker of osteoclast function. *Calcif. Tissue Int.* **34**, 285-290.

Moss, D. W., Eaton, R. H., Smith, J. K. and Whitby, L. G. (1967). Association of inorganic pyrophosphatase activity with human alkaline phosphatase preparations. *Biochem. J.* **102**, 53-57.

Nash, K., Feldmuller, M., de Jersey, J., Alewood, P. and Hamilton, S. (1993). Continuous and discontinuous assays for phosphotyrosyl protein phosphatase activity using phosphotyrosyl peptide substrates. *Anal. Biochem.* **213**, 303-309.

Oldberg, Å, Franzén, A. and Heinegård, D. (1986). Cloning and sequence analysis of rat bone sialoprotein (osteopontin) DNA reveals an Arg-Gly-Asp cell-binding sequence. *Proc. Natl. Acad. Sci. USA* **83**, 8819-8823.

Ornoy, A., Adomian, G. E. and Rimoin, D. L. (1985) Histologic and ultrastructural studies on the mineralisation process in hypophosphatasia. *Am. J. Med. Genet.* **22**, 743-758.

Parfitt, A. M. (1994). Osteonal and hemi-osteonal remodeling: the spatial and temporal framework for signal traffic in adult human bone. *J. Cell. Biochem.* **55**, 273-286.

Pevny, L., Simon, M. C., Robertson, E., Klein, W. H., Tsai, S-F, D'Agati, V., Orkin, S. H. and Constantine, F. (1991). Erythroid differentiation in chimaeric mice blocked by a targeted mutation in the gene for transcription factor GATA-1. *Nature* **349**, 257-260.

Piper, K. M., Boyde, A. and Jones, S. J. (1992). The relationship between the number of nuclei of an osteoclast and its resorptive capacity in vitro. *Anat. Embryol.* **186**, 291-299.

Que, L. Jr. and Scarrow, R. C. (1988). Active sites of binucelar iron-oxo proteins. *Am. Chem. Soc. Symp.* **372**, 152-178.

Reimold, A. M., Grusby, M. J., Kosaras, B., Fries, J. W. U., Mori, R., Maniwa, S., Clauss, I. M., Collins, T., Sidman, R. L. and Glimcher, L. H. (1996). Chondrodysplasia and neurological abnormalities in ATF-2-deficient mice. *Nature* **379**, 262-265.

Reinholt, F. P., Hultenby, K., Oldberg, Å. and Heinegård, D. (1990). Osteopontin – a possible anchor of osteoclasts to bone. *Proc. Natl. Acad. Sci. USA* **87**, 4473-4475.

Robison, R, (1923). The possible significance of hexosephosphoric esters in ossification. *Biochem. J.* **17**, 286-293.

Roodman, G. D., Ibbotson, K. J., MacDonald, B. F., Kuehl, H. J. and Mundy, G. R. (1985). 1,25(OH)$_2$ vitamin D$_3$ causes formation of multinucleated cells with osteoclastic characteristics in cultures of primate marrow. *Proc. Natl. Acad. Sci. USA* **82**, 8213-8217.

Sibille, J-C., Doi, K. and Aisen, P. (1987). Hydroxyl radical formation and iron-binding proteins. Stimulation by the purple acid phosphatases. *J. Biol. Chem.* **262**, 59-62.

Soriano, P., Montgomery, C., Geske, R. and Bradley, A. (1991). Targeted

disruption of the c-src proto-oncogene leads to osteopetrosis in mice. *Cell* **64**, 693-702.

Steinbeck, M. J., Appel, W. H., Verhoeven, A. J. and Karnovsky, M. J. (1994). NADPH-oxidase expression and in situ production of superoxide by osteoclasts actively resorbing bone. *J. Cell. Biol.* **126**, 765-772.

Sundquist, K. T., Cecchini, M. G. and Marks, S. C. (1995). Colony-stimulating factor-1 injections improve but do not cure skeletal sclerosis in osteopetrotic (op) mice. *Bone* **16**, 39-46.

Waymire, K. G., Mahuren, J. D., Jaje, J. M., Guilarte, T. R., Coburn, S. P. and McGregor, G. R. (1995). Mice lacking tissue non-specific alkaline phosphatase die from seizures due to defective metabolism of vitamin B-6. *Nature Genet.* **11**, 45-51.

Whyte, M. P. (1995). Hypophosphatasia. In *The Metabolic and Molecular Basis of Inherited Disease.* (ed. C. R. Scriver, A. L. Beaudet, W. S. Sly, D. Valle). 7th Edition, pp. 4095-4111. New York: McGraw-Hill

Wiktor-Jedrzejczak, W., Bartocci, A., Ferrante, A. W. J., Ahmed-Ansari, A., Sell, K. W., Pollard, J. W. and Stanley, E. R. (1990). Total absence of colony-stimulating factor 1 in the macrophage-deficient osteopetrotic (op/op) mouse. *Proc. Natl. Acad. Sci. USA* **87**, 4828-4832.